sustainability

MDPI

Article

Modelling of a Wave Energy Converter Impact on Coastal Erosion, a Case Study for Palm Beach-Azur, Algeria

Mehrdad Moradi *, Narimene Chertouk and Adrian Ilinca

Wind Energy Research Laboratory (WERL), Université du Québec à Rimouski, Rimouski, QC G5L 3A1, Canada
* Correspondence: mehrdad.moradi@uqar.ca; Tel.: +1-418-509-4589

Abstract: Facing the exhaustion of fossil energy and in the context of sustainable development, strong incentives are pushing for the development of renewable energies. Nuclear energy and fossil fuels like petroleum, coal, and natural gas provide most of the energy produced today. As a result, greenhouse gases are released and climate change becomes irreversible. Furthermore, radioactive waste disposal causes severe radiation pollution in nuclear power. Alternatives such as marine energy are more sustainable and predictable. It has none of the detrimental effects of fossil and nuclear energies and is significant in terms of environmental sustainability by defending the coastline from erosion. Here, we study the Palm Beach-Azur region near Algiers on the Mediterranean Sea. The study aims to use wave energy converters (WEC) to generate clean energy and reduce coastline erosion. The results of this study show that in the presence of wave energy converters, the wave height decreased by 0.3 m, and sediment deposition increased by 0.8 m. Thus, sand deposit prediction demonstrates that the presence of WEC decreases marine erosion and contributes to an accumulation of sediments on the coast. Moreover, this confirms that WECs can serve a dual role of extracting marine energy by converting it into electrical energy and as a defence against marine erosion. Therefore, WECs justify their efficiency both in energy production and economic and environmental profitability due to coastal protection.

Keywords: wave energy converters; erosion; SWAN model; wave height; energy dissipation

Citation: Moradi, M.; Chertouk, N.; Ilinca, A. Modelling of a Wave Energy Converter Impact on Coastal Erosion, a Case Study for Palm Beach-Azur, Algeria. *Sustainability* **2022**, *14*, 16595. https://doi.org/10.3390/su142416595

Academic Editors: Flora E. Karathanasi, Takvor Soukissian and Ioannis Kyriakides

Received: 17 October 2022
Accepted: 3 December 2022
Published: 11 December 2022

1. Introduction

Among the renewable energies experiencing considerable development, marine energies need more attention. The ocean, which covers 71% of the Earth's surface, is an underutilized energy source. The expected increase in the number and intensity of storms due to climate change, flooding along coastal areas, and the push for corporate environmental responsibility along coastal regions are opening the way for significant marine energy development. Wave Energy Converters (WEC) should be climate-proof (resistant to sea level rise and strong waves), environmentally friendly, and of low visual impact (submerged or low crested) to avoid negative impacts. Various WECs have different mechanisms and technologies for converting mechanical energy into electricity. These technologies have been reviewed by many authors [1–5].

Another vital feature of WECs is their influence on the hydrodynamics near coastlines. Various numerical and experimental studies have been conducted to assess the hydrodynamic impacts of coastal protection structures on nearshore flow characteristics. Atan et al. [6] have studied three arrays of configurations with 12 WECs on the western coasts of Ireland to measure the influence of these structures on nearshore wave climate and captured power. They found that wave height decreased by less than 1% between 1 km and 3 km from the coast and by 0.1% between 100–300 m from the coast. They also reported that wave power decreased by less than 1% between 1–3 km from the coast and by 0.2% between 100–300 m from the coastline.

Chang et al. [7] performed a sensitivity analysis of the SWAN (Simulating Waves Nearshore) model for WEC arrangements and features. They concluded that wave height decreases of 30% and 15% were observed because of two tested scenarios for wave energy converter structures. Flow regime alterations imposed by a wave farm located on the southwestern coasts of England were investigated using SWAN and ROMS (Regional Ocean Modeling System) models by Greaves & Iglesias [8]. They studied WECs effects on wave radiation stresses, bed shear stresses, bottom frictions, and sediment movement. The results confirmed that the wave farm influences gradients of bottom shear stress, which leads to adjusting current velocity, and wave heights (by around 5 to 10 cm). It has been reported that flow interactions and bed stress are the main factors affecting sediment transport patterns and subsequent morphological changes. Contardo et al. [9] validated their proposed SWAN model using measured field data from a series of wave measurement devices. Their model showed that WEC impacts on the wave field and flow structure are more significant at 40 m downstream of the unit, with a maximum drop of 20% of the wave height.

Apart from the impacts of WECs on the flow field and, consequently, the morphology of a region, it is also necessary to examine the region's potential in terms of wave energy. It can be considered the first step of the project implementation. Numerous studies have focused on the marine power potential of a region calculated from wave characteristics such as wave height and wave period [10–14]. The wave parameters are determined using in situ wave measurements, satellite data, and numerical wave models.

Appendini et al. [15] investigated the wave potential in the Caribbean Sea. To this end, they validated a 30-year wave hindcast of the region using altimetry (Globwave) and buoy (DIMAR) data. Based on their study, the Caribbean Low-Level Jet with easterly winds of 13 m/s has the highest potential for wave energy extraction with 8 to 14 kW/m. Garcia and Canals [16] assessed wave power potential in Puerto Rico and US Virgin Islands. They used a high-resolution wave model to estimate available wave power in the region. They reported 10 to 12 kW/m as the available potential of wave power, which reveals that these sites are theoretically appropriate for wave energy harvest projects.

The extractable wave energy of the Atlantic coast of Morocco was studied by Sierra et al. [17]. Using 44-year data series at 23 points and statistical analysis of significant wave heights, they categorized the domain of study in terms of the amount of recoverable energy. As a result, the central area of the Atlantic Moroccan coast, with the most considerable wave heights, was known as the optimal area for wave energy harvesting. This area had an annual average wave power higher than 25 kW/m.

The WECs use sensors which could pose several problems due to the possibility of simple disturbances causing errors. Future research should consider using interval observers instead of sensors. Based on the recent research by [18,19], interval observers can be used for control of linear and non-linear systems, and anti-disturbance controller design, in a wide range of applications such as Wave Energy Converters.

To maximize the benefits of WECs, installing them in the regions susceptible to coastal erosion is imperative. Beaches form about 20% of the planet's coastline. Of these, nearly 70% are undergoing a phase of erosion, 20% are stable, and 10% show signs of accumulation. Moreover, Choupin et al. [20] investigated the most significant factors affecting wave energy harvesting. As they noted local geographical specifications such as touristic features are critical in recognizing the suitable location for WEC installation. Algeria has a coastline of 1622 km, which welcomes millions of people. The beaches are a major tourist attraction, providing a primary economic interest and a natural landscape heritage of incomparable value. Since Algeria has a robust tourism industry, and considering its power demand and population density, these inputs justify the installation of WECs near its coasts. Unfortunately, this coastline is marked by degradation due to intensive erosion.

In this study, we focused on the area of Palm Beach-Azur, which constitutes a tourist site for summer visitors. High competition for using this natural environment has led to coastline degradation. Marked by long-term intensive erosion, this study evaluates the

shoreline's behaviour and the coastline's dynamics following the installation of WECs. In addition, it determines the effect of this equipment on the hydrodynamics.

2. Materials and Methods

2.1. SWAN Mathematical Model

In this study, SWAN has been used to calculate wave height reduction and energy dissipation due to the design of the wave farm. SWAN is a third-generation wave model developed by Booij et al. [21] that estimates wave characteristics (significant wave height, peak period, average direction, and the spectrum of directional waves) in coastal areas, lakes, and estuaries. The required inputs are wind data, the bathymetry of the region, and flow input information. The model solves the equilibrium equation of the action of the spectral waves without prior assumptions on the shape of the wave spectrum. A two-dimensional wave action density spectrum, $N(\omega, \theta)$, describes the wave field, where ω is the angular wave frequency, and θ is the direction of the wave. The wave action density spectrum is used instead of the energy density spectrum. The action density is conserved in the presence of currents, but the energy density is not. Therefore, the wave energy spectrum can be calculated from the wave action spectrum. The wave action equilibrium equation is discretized using A time-based method of finite difference, geographic space (x, y), and spectral space (ω, θ). The equilibrium equation of the action of the spectral waves is:

$$\frac{\partial N}{\partial t} + \frac{\partial (c_x N)}{\partial x} + \frac{\partial (c_y N)}{\partial y} + \frac{\partial (c_\omega N)}{\partial \omega} + \frac{\partial (c_\theta N)}{\partial \theta} = \frac{S}{\omega} \quad (1)$$

The first term indicates the local change rate in wave action density on the left-hand side of the equation. The second and third terms refer to the action of waves over a geographical space, with their propagation speed and direction, respectively. The fourth term quantifies the relative frequency shift due to variations in depths and currents, with a propagation speed of c_x and c_y in the X and Y directions. Finally, the fifth term represents the refractive effects induced by depth variations or currents, with propagation speed c_θ in the direction θ. The explanations of propagation velocity above stem from linear wave theory. Considering the right side of the equation, S refers to the source and sink terms in the physical processes that produce, dissipate, or redistribute wave energy:

$$S = S_{nl4} + S_{nl3} + S_{in} + S_{wc} + S_{bot} + S_{brk} \quad (2)$$

Here, S_{nl4} presents to the redistribution of energy by nonlinear quadruplet wave-wave interactions, S_{nl3} refers to the redistribution of the nonlinear triad of wave energy, S_{in} is the transfer of wind energy to waves and the dissipation of wave energy that occurs as a result of white capping, S_{bot} is the term for background friction energy elimination, and S_{brk} is the random wave energy dissipation due to depth-induced fracture.

The wave energy flow, also called wave power, is calculated on its X and Y components with the following two expressions:

$$J_x = \iint_0^{2\pi} \rho g c_x E(\sigma, \theta) d\sigma d\theta \quad (3)$$

$$J_y = \iint_0^{2\pi} \rho g c_y E(\sigma, \theta) d\sigma d\theta \quad (4)$$

where $E(\sigma, \theta)$ is the directional spectral density, which specifies how energy is distributed over frequencies (σ) and directions (θ). The magnitude of the wave power is then calculated as follows:

$$J = \left(J_x^2 + J_y^2 \right)^{\frac{1}{2}} \quad (5)$$

SWAN model documentation [22] describes the set of equations governing the spectral distribution of wind waves, the transmission of wave energy, the source and sinks, the

effect of the ambient current on the waves, the modelling of obstacles and structures, and the configuration induced by the waves.

2.2. Wave Refraction Calculation

Approaching the coast and from a certain depth (according to the linear theory d = $1/2L_0$, i.e., the half-wavelength of the offshore swell), the propagation of swells is influenced by the bathymetry. As a result, wave ridges tend to become parallel to isobaths. This phenomenon is called wave refraction. This way, the energy is concentrated on the salient (heading, arrows, etc.) and spread out on the re-entrants (creeks, gulfs, etc.). The study of refraction seeks to unravel the characteristics of the swell (direction and height) as it propagates from the open sea toward the coast.

The wave refraction phenomenon is accounted for by calculating the refraction coefficients (K_r) at several points on a coastline for the dominant swell sectors and a given swell period. Thus, we opt to calculate the Shoalling Coefficient K_s.

$$K_s = \frac{H_s\ (Certain\ location)}{H_s\ (Deep\ water)} \tag{6}$$

The values of K_s calculated up to the coast reflect the following:

- The energy attenuation when $K_s < 1$ (wave divergence);
- The conservation of energy when $K_s = 1$ (rectilinear wave propagation);
- The concentration of energy when $K_s > 1$ (convergence of waves).

The calculations of the refraction of the swell between the open sea and the coast are carried out by the digital SWAN model.

Application of the Model

The software models the propagation of the swell by considering these phenomena:

- Refraction on the bottoms and around the structures;
- Friction on the bottom;
- Surge.

The best practice for effectively applying the model is using a smaller grid according to the area of study. Meshing is very important to reduce computation time and improve accuracy. In this study, the calculations were performed first on a coarse grid for a larger region, and then the results were used as boundary conditions for a finer grid. The grid has 31 rows, 28 columns, and 868 nodes, and the mesh dimensions are X = 2.7 m and Y = 36.65 m.

Meshing must be performed using Cartesian or Spherical coordinates. Additionally, SWAN can also simulate grids that are irregular, and consists of triangles or tetrahedra in an irregular pattern. It is helpful for shorelines with irregular contours and complex bottom topographies. Therefore, since the calculations are performed on a grid, SWAN is an Eulerian model that considers the refractive propagation over different bathymetries and flow fields. This model solves the discrete equilibrium equation. SWAN represents the directional and non-directional spectrum at any point of the computing grids through spectral and time-dependent wave characteristics, such as wave height, maximum or average period, wave direction, and energy transport.

The SWAN simulations in this study are carried out using two computational grids, a coarse offshore-to-shore grid and a high-resolution grid in the local region of interest. The resolution of the nested grid allows the precise definition of the WEC position in the array and the precise simulation of their operation. For a detailed assessment of the impacts of the wave farm, this is a prerequisite, as mentioned by Carballo and Iglesias [23].

2.3. Bathymetry Data

The bathymetry used for the refraction study is that taken from the (GEBCO, n.d.) website [24]. The bathymetry was extracted as a table using the SURFER software. To

improve accuracy, for the coastal zone between −22 m up to 0 m, the data extracted from the GEBCO website was replaced by the data obtained during the in situ bathymetry measurement (2016). Figure 1 represents the bathymetric data of the Palm-Beach Azur zone in the SURFER software.

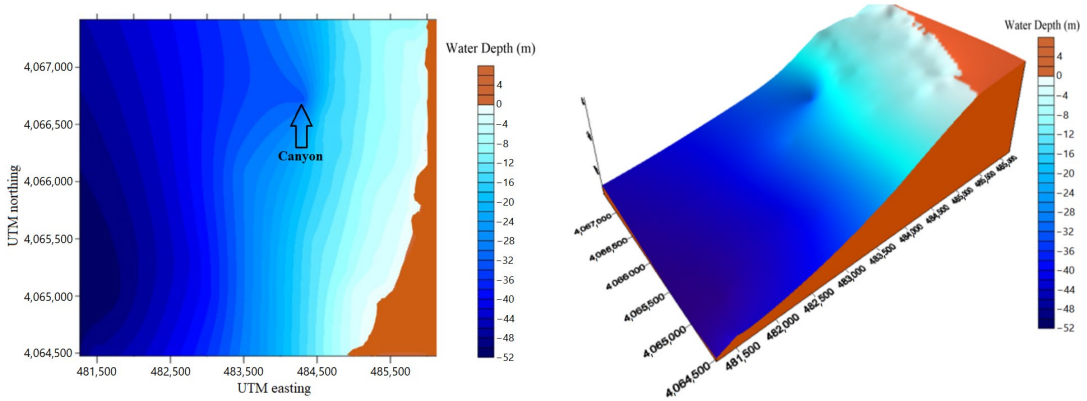

Figure 1. The bathymetric map of Palm Beach-Azur.

As shown in Figure 1, the contour lines are regular and parallel to the coast coming towards the coast and more spaced going towards the open sea, with the presence of a canyon, which means a fall to the depth of −23 m on the Northeast side. The general average slope of the bottom is of the order of 1%.

Two bathymetric grids were prepared, a large grid that covers deep water depths up to −100 m and a small grid of −50 m. In this study, the −50 m grid is of interest. The −100 m grid is only used to determine the characteristics of the swell in the −50 m grid. Once the bathymetry map was projected by SURFER (v18.1.186) software, the bathymetry was extracted for all the grid points. The depths were recorded as (.dat) files. Then, they were incorporated into MATLAB and imported into the SWAN model.

2.4. Offshore Swell Data

The offshore swell data used for the refraction calculation is from the Summary of Synoptic Meteorological Observations (SSMO) [25], consisting of ships' observations from 1963 to 1970. Statistical processing of these data provided the frequencies of swells' appearance by direction and period. The periods were chosen according to the probability distribution of exceeding a swell of a given amplitude. Swells of high amplitude have a relatively low probability of occurrence. Table 1 relates the swell conditions used in the context of this study.

Table 1. The characteristics of the decadal swells used in the SWAN model.

Offshore Swell Direction	Peak Period (S)	Significant Height Offshore (m)
N 340°	8	6.8
N 30°	9	7
N 280°	10	8

2.5. WEC Type and Integration Data

We used the same method as Carballo and Iglesias [23] to determine the effects of WECs installation on the erosion of the Palm Beach-Azur. The WEC we use is the WaveCat illustrated in Figure 2 [26]. It is a floating WEC whose operating principle is oblique overtopping. It should be deployed at sea (in 50–100 m of water) and produces a limited impact on the shoreline. It is composed of two convergent hulls with a single-point mooring to a Catenary Anchor Leg Mooring (CALM) buoy which allows the device to orient itself passively with the direction of wave propagation. The WaveCat's bows are kept afloat, and incoming waves propagate through the space between the hulls. When the wave

crests overtake the inner sides of the hull, the overflowing water is collected in tanks at a level above the external sea level. Then, the water is discharged to the sea and drives turbine-generator units. The device acts as a single-shell body by reducing the angle to 0° and effectively closing.

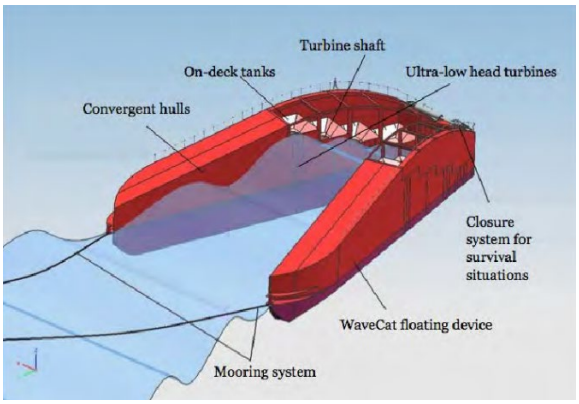

Figure 2. Schematic of the WaveCat energy converter [26].

To study the impact on beach erosion, we are introducing 13 WaveCat Overtopping converters arranged in 2 parallel rows, the nearshore row having 7 WECs and the offshore row containing 6 WECs (Figure 3). The WECs are installed at a depth of 20 m, and the distance between them is 2.2 times the distance D. A WaveCat's distance D is 45 m between its two most distant arcs. The WEC-wave field interaction is modelled using the transmission coefficients of the waves obtained during laboratory tests carried out at the Porto laboratory by Fernandez et al. [26]. As a result of various wave conditions, the transmission coefficients are calculated as a ratio between the wave heights measured downwind and in front of the WEC. The results showed that the wave transmission coefficient exhibited very low variability (K_t = 0.76). Consequently, medium- and long-term analyses use constant values.. Furthermore, the limited range of wave conditions prevented the development of a frequency-dependent model.

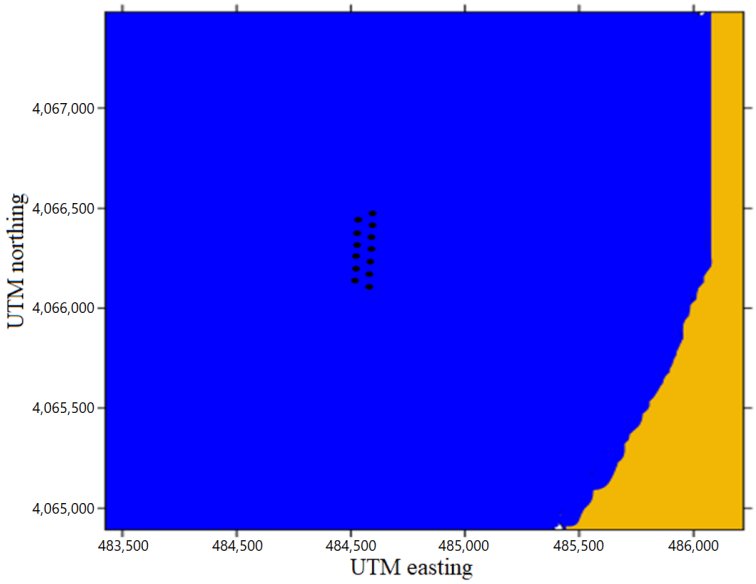

Figure 3. WEC location configuration in the study area.

3. Zone of Study

3.1. Geographical Location

The Bay of Bou Ismail, formerly Castiglione, is one of the most prominent bays on the Algerian coast. It is located in the central part of the Algerian coast, 50 km west of Algiers, in the Tipaza region. It is between 2°25′ in the west and 2°55′ in the east. The Palm Beach-Azur area is in the eastern sector of the bay of Bou-Ismaïl in the municipality of Zéralda, about 27 km west of Algiers, extends over 2000 m. It is bordered to the west by the Mediterranean Sea, to the east by the municipality of Zéralda, to the north by the presidential port, and to the south by the transverse groin and the breakwaters of the tourist complex of Zéralda (Figure 4). This area is important because of its proximity to the capital city and opening to the Mediterranean Sea. As a result, it is an object of interest and a point of attraction for tourists. Therefore, its protection from coastal erosion is very important.

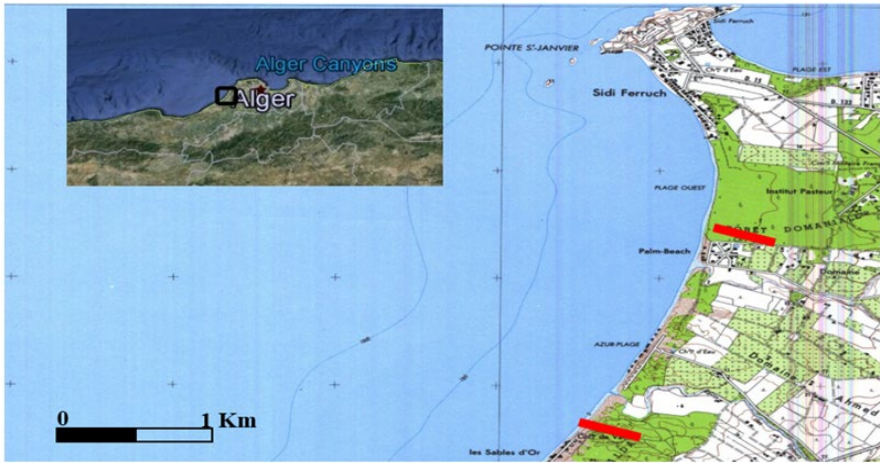

Figure 4. Geographical location of the Palm Beach-Azur area [27].

3.2. Sedimentology of The Zone of Study

The bay of Bou Ismail is characterized by a diverse sedimentological texture based on nine facies: fine sands, fine silty sands, sandy silts, gravelly sands, silted gravies, coarse sands, fine gravels, pure, and rocky. As illustrated in Figure 5, the coastal zone of Palm Beach-Azur is dominated by fine and coarse sand from 0 to 20 m. Below this depth, sandy and pure silt dominates the zone until 100 m deep, where the silted gravel appears.

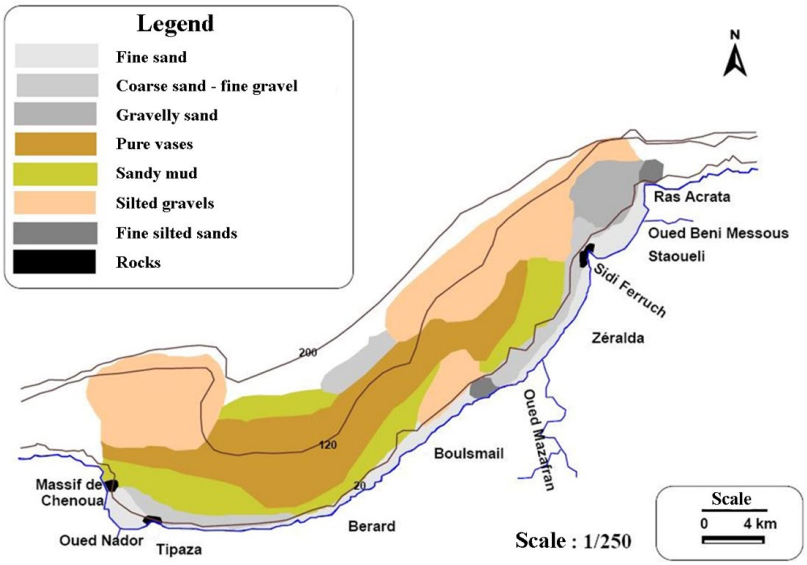

Figure 5. Sedimentology of the bay of Bou-Ismail [28].

3.3. Climate and Wind Data

Wind generates waves and currents, and their impacts increase with their speeds. When the action of the winds is continuous, they generate swells. In the bay of Bou-Ismail, the distribution of the winds is ideally linked to the annual swell regime. The data collected by the SSMO (Summary of Synoptic Meteorological Observations) off the coast of Algeria confirms the existence of two distinct periods:

I. A winter period (October-March), with prevailing winds from the west, with a frequency ranging from 60 to 80%;
II. During summer (April-September), the prevailing winds are from the east and the northeast, with 45 to 75% frequencies for the northeast direction.

Figure 6 depicts the annual distribution of wind in the zone of study. Winds from the West (W) direction have an average maximum speed (average extreme winds) of 19.5 m/s.

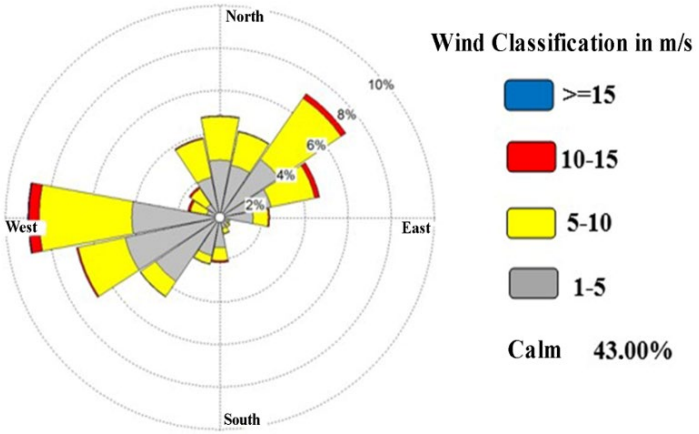

Figure 6. Annual wind distribution in percent, Dar-El-Beida province, 1995–2015 [29].

3.4. The Sea Swells

The swell characteristics determine the sedimentary displacement in the breaking zone, the volume and the direction of the sediment transit, and its incidence on the coast. These characteristics condition the dimensioning of the coastal protection structure and its implantation. The primary data source is the SSMO (Summary of Synoptic Meteologic Observations) data in the Algiers region, conducted by the U.S Naval weather service Command [25]. The monthly wave frequencies analysis shows that:

- The highest appearance frequencies are related to those swells from the west, east, and northeast. The weakest ones are recorded for swells in the north and north-west directions;
- The frequencies of observations over the year of the easterly and westerly swells are roughly identical. However, a slight predominance of the eastern sector exists.

Storm swells mainly come from the western sector.

From Figure 7, we conclude that the swell distribution is generally consistent with the wind regime:

I. In winter: western swells dominate with the majority of amplitudes of 1 and 3 m and can reach up to 4 m;
II. In summer: The most dominant swells come from the northeast sector with smaller amplitudes, and the swells from the west are quite significant.

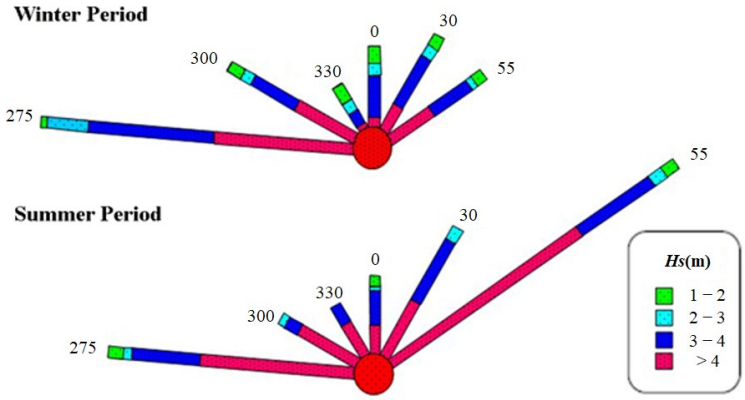

Figure 7. Swell direction summary roses off the sector (275°–55°) [30].

4. Results

4.1. Wave Modelling

Several tests illustrate the wave propagation, but we chose to present the most significant case, with a wave height *Hs* = 8 m, period *T* = 10 s, and direction of 280° N, without integrating WECs in the grid (Case 1). The SWAN model allowed us to obtain results shown in Figure 8. It shows the propagation of the sea swell towards the coast on the large grid, coming from water depth of more than 100 m. The wave depth contours are regular and parallel to the coast. Therefore, the wave direction is perpendicular to the coast.

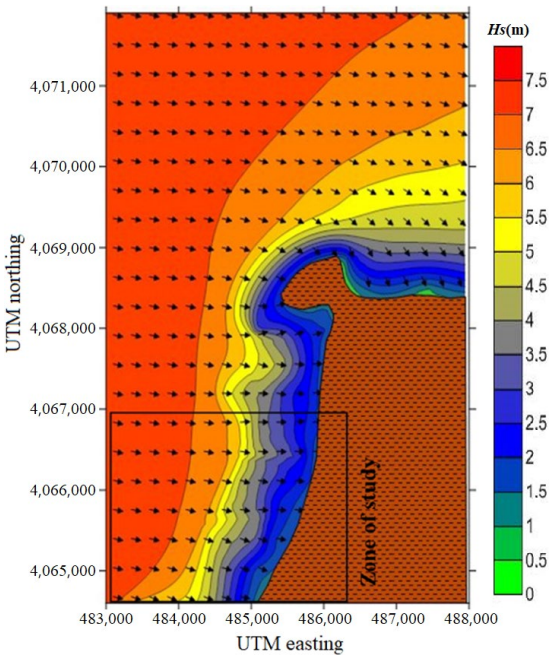

Figure 8. Wave refraction for a direction of 280° N and a wave period of 10 s.

Figure 9 shows the small grid for depths of 50 m. The computation uses the swells calculated from the large grid as boundary and initial conditions. West-trending swells are the most energetic in the area, so they are presented here. Their propagation is perpendicular to the Palm Beach-Azur shoreline because of the region's morphology perpendicular to that direction. This study found that the swell conditions within 50 m were as follows: wave direction = 280° N, significant wave height (*Hs*) = 5 m, and wave period (*T*) = 7 s. The results are presented on the following maps:

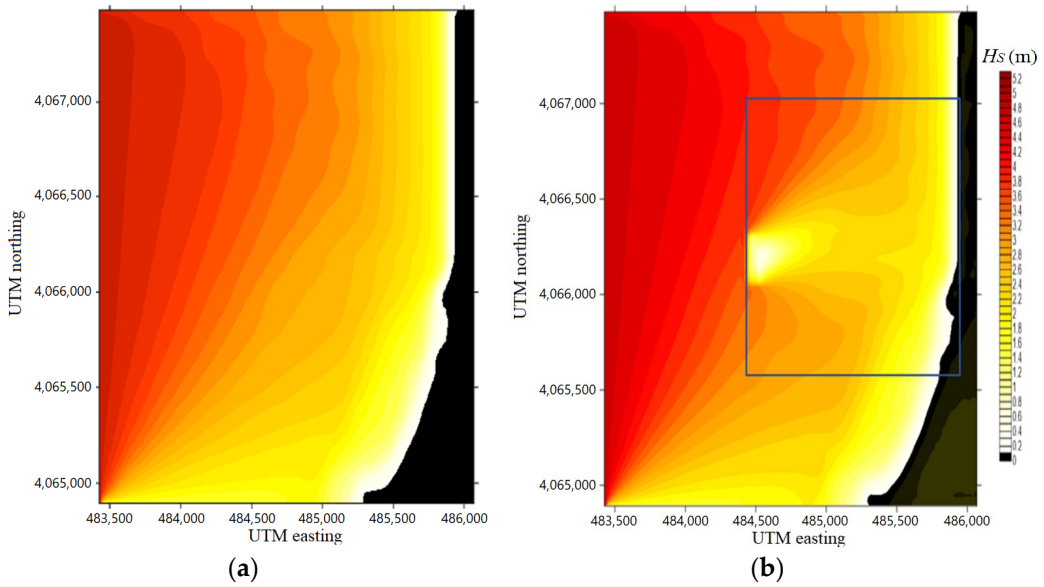

Figure 9. Contours of *Hs* obtained using the SWAN model for a direction of 280° N, *Hs* = 5 m, and *T* = 7s: (**a**) before the integration of the WECs; (**b**) after the integration of the WECs.

In Figure 9a, without WECs, we have regular isolines of *Hs*. The wave height decreases in the presence of WECs (Figure 9b), mainly at the WECs level, and continues up to the coast. At the WECs' level, the *Hs* was 1.1 m instead of 3.6 m, and it continues to decrease along its path until it arrives at the coast with zero depth. With the decrease in *Hs*, we can see that WECs can dissipate energy, demonstrating their potential for energy production and coastline protection.

An area was selected to calculate the Δ*Hs*, and precisely observe the impacts of WECs on wave height. This zone is depicted in Figure 9b. In this area, the significant wave height *Hs* and the Δ*Hs* between the two cases were calculated and presented in Table 2. As we notice from the wave height data analysis, there is a decrease in the mean value of *Hs* by Δ*Hs* = 0.3 m. That represents a 30% decrease in the height of the significant waves in the area. The Shoaling Coefficient also confirms this. After installing WECs, the wave field will diverge more due to the change in the Shoaling Coefficient (*Ks*). *Ks* at 10 m depth, on average, equals 0.512 without WEC and 0.452 with WEC, where these swells reach the coastline without changing direction. As they approach the coast, the swells only lose a fraction of their enormous energy. The energy dissipation is pivoting the orthogonal in a northwest to west direction. We measure an average angle of 280.08° and 282.41°, respectively, after and before WEC installation.

Table 2. The mean Δ*Hs* and the Shoaling Coefficient for two cases of no WECs and with WECs.

Parameters	No WECs	With WECs
Average of *Hs* (m)	2.56	2.26
Average Δ*Hs* (m)	0.3	
Average Δ*Hs* (%)	30%	
Shoaling Coefficient *Ks*	0.512	0.452

4.2. Sedimentation Pattern near Wave Energy Converters

The profiles closest to the WEC integration zone plotted in Figure 10 illustrate the influence of the WEC on the bathymetric profile. We superimposed the maps of the two cases (with and without WECs) to draw the sedimentation profile from the WECs' location towards the shore.

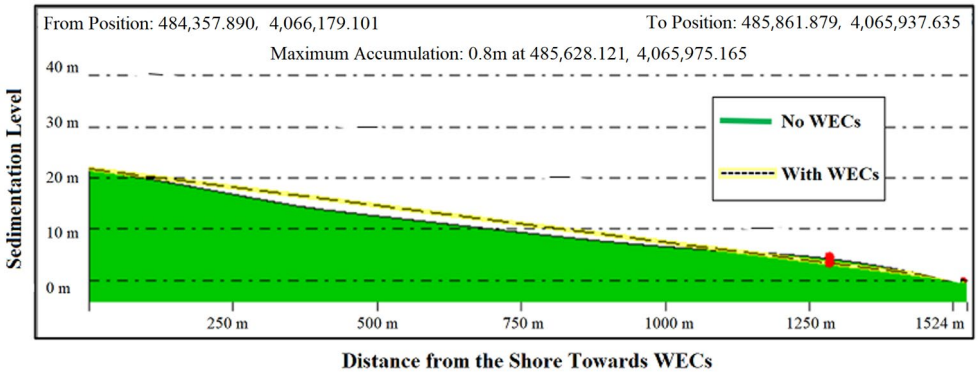

Figure 10. Sedimentation profiles for no WECs and with WECs.

As seen in Figure 10, there is a distinctive difference between the two bathymetric profiles, as displayed by no WECs diagram being below the case with WECs. There is an accumulation after the installation of the WEC, with a maximum accumulation of 0.8 m. This bathymetric change is the result of the decrease in significant wave height (*Hs*) and energy dissipation near WECs. Therefore, we can deduce that the installation of the WEC can serve a dual role, the extraction of marine energy to convert it into electrical energy and the protection of coasts against marine erosion according to the results of sediment deposition of 0.8 m at the provided coordination.

5. Conclusions

Waves have the potential to provide a sustainable source of energy that can be transformed through energy converters into electrical energy in shallow or deep water. Erosion is a natural phenomenon mainly linked to meteorological and hydrodynamic effects. In addition, the human influence on the shore accelerates and worsens erosion patterns in coastal regions.

Palm Beach-Azur, the subject of this study, is located in the eastern part of the Bay of Bou Ismaïl. It is one of the most significant beaches on the Algerian coast. This study aimed to investigate the effect of WaveCat Wave Energy Converters (WECs) on wave hydrodynamics and marine erosion.

In this study, the presence of WECs correlated to a decrease in the shoaling coefficient, confirming that the WECs captured wave energy as wave heights declined. Moreover, it has been seen that the WECs changed the bathymetric profile so that an accumulation of sediment appeared. Therefore, we conclude that WECs can be used to protect shorelines from marine erosion while transforming wave energy into electrical power.

As observed, WECs can play a dual role in power generation and coastline protection, yet their economic feasibility still poses an issue. However, the high installation cost of WECs can be justified when considering they eliminate the need for the construction of erosion protection structures.

Author Contributions: Conceptualization, M.M., N.C. and A.I.; methodology, N.C. and M.M.; software, N.C.; validation, M.M. and N.C.; writing—original draft preparation, M.M. and N.C.; writing—review and editing, A.I.; visualization, M.M. and N.C.; supervision, A.I. All authors have read and agreed to the published version of the manuscript.

Funding: This research was funded by NSERC (Canada) through a discovery grant.

Institutional Review Board Statement: Not applicable.

Informed Consent Statement: Not applicable.

Data Availability Statement: Not applicable.

Conflicts of Interest: The authors declare no conflict of interest.

References

1. Drew, B.; Plummer, A.R.; Sahinkaya, M.N. A review of wave energy converter technology. *Proc. Inst. Mech. Eng. Part A J. Power Energy* **2009**, *223*, 887–902. [CrossRef]
2. Antonio, F.D.O. Wave energy utilization: A review of the technologies. *Renew. Sustain. Energy Rev.* **2010**, *14*, 899–918.
3. Falnes, J. A review of wave-energy extraction. *Mar. Struct.* **2007**, *20*, 185–201. [CrossRef]
4. McCormick, M.E. *Ocean Wave Energy Conversion*; Dover Publications: Mineola, NY, USA, 2007; p. 233.
5. Thorpe, T.W. A brief review of wave energy. In *Harwell Laboratory, Energy Technology Support Unit*; AEA Technology: UK, 1999.
6. Atan, R.; Finnegan, W.; Nash, S.; Goggins, J. The effect of arrays of wave energy converters on the nearshore wave climate. *Ocean Eng.* **2019**, *172*, 373–384. [CrossRef]
7. Chang, G.; Ruehl, K.; Jones, C.A.; Roberts, J.; Chartrand, C. Numerical modeling of the effects of wave energy converter characteristics on nearshore wave conditions. *Renew. Energy* **2016**, *89*, 636–648. [CrossRef]
8. Greaves, D.; Iglesias, G. Wave and tidal energy. In *Wave and Tidal Energy*; John Wiley & Sons: Hoboken, NJ, USA, 2017.
9. Contardo, S.; Hoeke, R.; Hemer, M.; Symonds, G.; McInnes, K.; O'Grady, J. In situ observations and simulations of coastal wave field transformation by wave energy converters. *Coast. Eng.* **2018**, *140*, 175–188. [CrossRef]
10. Gonçalves, M.; Martinho, P.; Guedes Soares, C. Wave energy conditions in the western French coast. *Renew. Energy* **2014**, *62*, 155–163. [CrossRef]
11. Guillou, N.; Chapalain, G. Numerical modelling of nearshore wave energy resource in the Sea of Iroise. *Renew. Energy* **2015**, *83*, 942–953. [CrossRef]
12. Iglesias, G.; López, M.; Carballo, R.; Castro, A.; Fraguela, J.A.; Frigaard, P. Wave energy potential in Galicia (NW Spain). *Renew. Energy* **2009**, *34*, 2323–2333. [CrossRef]
13. Iglesias, G.; Carballo, R. Wave energy potential along the Death Coast (Spain). *Energy* **2009**, *34*, 1963–1975. [CrossRef]
14. Mendes, R.P.G.; Calado, M.R.A.; Mariano, S.J.P.S. Wave energy potential in Portugal–Assessment based on probabilistic description of ocean waves parameters. *Renew. Energy* **2012**, *47*, 1–8. [CrossRef]
15. Appendini, C.M.; Urbano-Latorre, C.P.; Figueroa, B.; Dagua-Paz, C.J.; Torres-Freyermuth, A.; Salles, P. Wave energy potential assessment in the Caribbean Low Level Jet using wave hindcast information. *Appl. Energy* **2015**, *137*, 375–384. [CrossRef]
16. Garcia, C.; Canals, M. Wave energy resource assessment and recoverable wave energy in Puerto Rico and the US Virgin Islands. In Proceedings of the MTS/IEEE OCEANS 2015—Genova: Discovering Sustainable Ocean Energy for a New World, Genova, Italy, 18–21 May 2015.
17. Sierra, J.P.; Martín, C.; Mösso, C.; Mestres, M.; Jebbad, R. Wave energy potential along the Atlantic coast of Morocco. *Renew. Energy* **2016**, *96*, 20–32. [CrossRef]
18. Khan, A.; Xie, W.; Zhang, B.; Liu, L.W. A survey of interval observers design methods and implementation for uncertain systems. *J. Frankl. Inst.* **2021**, *358*, 3077–3126. [CrossRef]
19. Khan, A.; Xie, W.; Liu, L.W. Set-membership interval state estimator design using observability matrix for discrete-time switched linear systems. *IEEE Sens. J.* **2020**, *20*, 6121–6129. [CrossRef]
20. Choupin, O.; Andutta, F.P.; Etemad-Shahidi, A.; Tomlinson, R. A decision-making process for wave energy converter and location pairing. *Renew. Sustain. Energy Rev.* **2021**, *147*, 111225. [CrossRef]
21. Booij, N.; Ris, R.C.; Holthuijsen, L.H. A third-generation wave model for coastal regions: 1. Model description and validation. *J. Geophys. Res. Ocean.* **1999**, *104*, 7649–7666. [CrossRef]
22. SWAN Team—SWAN User Manual, Delft University of Technology. 2022. Available online: https://swanmodel.sourceforge.io/ (accessed on 11 October 2022).
23. Carballo, R.; Iglesias, G. Wave farm impact based on realistic wave-WEC interaction. *Energy* **2013**, *51*, 216–229. [CrossRef]
24. GEBCO. (n.d.). GEBCO—The General Bathymetric Chart of the Oceans. Available online: https://www.gebco.net/ (accessed on 6 January 2022).
25. SSMO. *Summary of Synoptic Meteologic Observations: Mediteranean Marine Areas*; U.S Naval weather service Command: Kiln, MS, USA, 1970; Volume 2, 632p.
26. Fernandez, H.; Iglesias, G.; Carballo, R.; Castro, A.; Fraguela, J.A.; Taveira-Pinto, F.; Sanchez, M. The new wave energy converter WaveCat: Concept and laboratory tests. *Mar. Struct.* **2012**, *29*, 58–70. [CrossRef]
27. Belkacem, Y. Intégration des Mesures in situ et des Données Satellitaires dans un Système D'information Géographique pour Caractériser les eaux Côtières. Ph.D. Thesis, University of sciences and technology Hourai-Boumedien, Algiers, Algeria, 2010.
28. LEM (Laboratoire des Études Maritimes). *Etude de Délimitation d'une Zone d'extraction de Sable sur la Baie d'Alger*; Maritime Studies Laboratory of Algeria: Algiers, Algeria, 1998.
29. National Office of Meteorology. Available online: https://www.aps.dz (accessed on 10 January 2021).
30. Zemenzer, S. *Ensablement du port par transport sédimentaire simulation et application du modèle de Gao et Collins (1994) au port de Sidi Fredj*; Mémoire d'ingéniorat, Institut de Sciences de la Mer et de l'Aménagement du Littoral: Dély Ibrahim, Alger, 2004.